Regular Paper

Air Flow Channel Planning for Droplet-Spray-Type Olfactory Displays Using a Small Wind Tunnel

Yohei Seta[*,***], Mitsunori Makino[**], Yuichi Bannai[***], and Motofumi Hattori[***]

[*]Graduate School of Science and Engineering, Chuo University, Japan
[**]Faculty of Science and Engineering, Chuo University, Japan
[***]Department of Information Media, Kanagawa Institute of Technology, Japan
{a15.s845, makino.fme7}@g.chuo-u.ac.jp
{bannai, hattori}@ic.kanagawa-it.ac.jp

Abstract - To develop an olfactory display with high fragrance presentation performance and ease of maintenance for long-term use, a small wind tunnel was constructed to observe the inside of the flow channel of a prototype with a piezoelectric droplet spray mechanism for solving the problem of poor volatilization of the fragrance solution in the flow channel. The cross-sectional dimensions of the flow channel minimize the time for visible droplets to exist in the channel after purified water is sprayed in a small wind tunnel, where the channel height and width can be changed.

Spraying was performed on the obtained cross-sectional dimensions in five fragrance solutions, and no volatilization defects were observed in all but one of them. The piezoelectric olfactory display with the cross-sectional dimensions of the flow path obtained in this study is expected to contribute to the development of olfactory displays that can precisely synchronize the aroma with video and audio information.

Keywords: olfactory display, pulse ejection, droplet atomization, visualization

1 INTRODUCTION

Among the devices that present stimuli to people's five senses, a device that presents visual stimuli is called a display, whereas a device that presents olfactory stimuli is called an Olfactory Display. In 1962, the Sensorama [1] was the first known example of an olfactory display. Since the 1990s, multimodal interfaces have been actively researched in the field of human interfaces, and interest in the five senses of people has increased [2]. Various types of olfactory displays have been developed since the 2000s [3]-[4], and their applications include a system that presents smells synchronized with TV images and movies, with smells shown in movie theaters [5]. In virtual reality, by presenting sensory stimuli in addition to visual and auditory stimuli, users can experience smells in a VR environment [6].

Olfactory displays can be broadly classified into two types: those that control the injection of air mixed with fragrance components in advance and those that atomize solutions containing fragrance components as tiny droplets and vaporize them in air at room temperature. In either format, the user inhales air-containing fragrance components to allow them to reach the olfactory cells in the nasal cavity, thereby enabling the presentation of fragrance information [7].

When presenting an odor synchronized with video or VR content, if a high concentration of odor is continuously given that everyone can recognize, the odor will remain in the space, which is a residual problem [8]. If another odor is present in a residual state, the odor will be mixed up. Another problem is olfactory adaptation, which is the inability to perceive odors when the odor stimuli are administered on a sustained basis.

To solve these problems, Okada et al. developed an inkjet olfactory display [9] that used a thermal inkjet printer head to spray fragrance droplets. This is characterized by the fact that several hundred microscopic holes in the printer head eject several picoliters of droplets at a frequency of several KHz, enabling accurate control of the ejection volume and density over a wide dynamic range.

To confirm the basic performance of this olfactory display, experiments were conducted on the sensory characteristics of smell through subjective evaluation, and the following findings were obtained: Kadowaki et al. showed that humans could adequately perceive fragrances when pulsed fragrances were presented by injection for a very short period (approximately 0.1 s). They noted that this allowed the experiment to be conducted with a very small amount of aroma injection, thereby reducing the residual aroma in the air [10]. In addition, although the human sense of smell adapts to aroma stimuli in a short period of time, it is possible to reduce the onset of olfactory adaptation by presenting minute amounts of aroma in a pulsed (intermittent) form [11]. Noguchi et al. showed that there is a time threshold for the fragrance injection interval at which two pulsed fragrances can be perceived separately during one breath (two-point fragrance separation threshold) [12]. Based on the results of olfactory sensitivity measurements over time within one breath, they proposed an injection method that maximizes the perceived fragrance intensity during one breath. Aruga et al. proposed a method to measure scent discrimination thresholds using a pairwise comparison of two scent pulses as a measure of olfactory sensitivity, and applied it to an experiment to investigate the effect of self-motion sensation on olfactory sensitivity [13].

These findings indicate that pulse injection of scents is more effective than continuous presentation of scents in

synchronization with other information media [9]. Thus, the inkjet olfactory display is superior in terms of granularity and precision of injection volume and injection time, and can be said to have a sufficient level of performance for olfactory displays. Although ink cartridges are commercially available, they are black boxes and cannot be disassembled and cleaned to deal with head clogging and odors over long periods of use, which is a maintenance problem [8]. This problem may cause inkjet olfactory displays that have been used for a long period of time to receive extra fragrance components, even when fragrances are not present, leading to a decline in fragrance switching performance and experimental accuracy. In addition, in thermal inkjet printers, the heat from the heater creates bubbles in the liquid, which push out droplets through pressure changes, and there are concerns regarding the effect on heat-sensitive fragrances. Printer manufacturers hold patents for inkjet technology, including technologies for preventing head clogging and removing clogging, and there are significant obstacles to the development of olfactory displays using new inkjet engines in the future.

Therefore, for the practical application of olfactory displays based on open technology, this research group is conducting research and development of a new olfactory display focusing on spraying droplets using the ultrasonic vibration of a piezoelectric element with microscopic holes [14], aiming at precise droplet spraying based on a simpler principle. In this study, this is referred to as a piezoelectric olfactory display. The piezoelectric olfactory display is intended to be applied not only to VR content but also to a wide range of fields, such as psychophysical experiments, by achieving both a pulse injection performance of fragrance equivalent to that of the inkjet type and maintainability that allows long-term use.

In this process, a prototype was made following the body channel dimensions used for the inkjet-type [15]. When the prototype was sprayed with droplets for a short period to evaluate its performance, droplet adhesion on the bottom surface of the channel was confirmed [16]. The droplets were confirmed to vaporize afterwards, but some droplets remained for a few seconds after the end of droplet spraying. This indicates the possibility of continuous scent presentation for more than ten times the time of droplet atomization. This problem must be solved to achieve a pulse injection performance of a fragrance equivalent to that of an inkjet-type.

Possible solutions to this problem include changing to a more volatile fragrance solution, reducing the diameter of the sprayed droplets to improve their surface area, increasing the volatility, and expanding the flow path shape such that the sprayed droplets do not contact each other until they fully evaporate. In the case of a change in the fragrance of a solution, a change in its physical properties may interfere with the atomization of the piezoelectric element. In addition, to reduce droplet diameter, it is necessary to perforate the piezoelectric element mold with micropores of different sizes. When changing the shape of the flow path, it is necessary to find a flow path dimension that is sufficiently volatile, even if the atomizing object comes into contact with it; however, this will lead to a larger body.

In this study, we employed a change in channel geometry, which has the lowest change cost among the above approaches, to obtain the necessary and sufficient channel cross-sectional dimensions without droplet adhesion during droplet spraying. An experimental wind tunnel with variable channel walls was constructed to allow direct observation of droplet volatilization failure in the channel. In the experimental wind tunnel, the structure was created using fluid dynamics to achieve a stable and unbiased airflow inside the tunnel [17]-[18]. Based on the hypothesis that if there is no droplet adhesion in purified water, there will be no droplet adhesion in fragrance solutions containing a portion of ethanol. We will conduct a purified water spray experiment while moving along the channel wall and confirm whether there is droplet adhesion by visually observing and extracting the sprayed object from the video captured using image processing technology. When the flow dimensions without droplet adhesion of water were obtained, the effectiveness was verified by injecting a fragrance solution with the same dimensions. By creating a piezoelectric olfactory display with the obtained channel dimensions, we expect to make progress in the development of an olfactory display with a droplet spray mechanism that is easy to maintain and has the same pulse injection performance as an inkjet-type fragrance solution and easy removal of fragrance.

2 METHODOLOGY

2.1 Piezoelectric Olfactory Display

Our research group developed a piezoelectric olfactory display that adopts a piezoelectric element as a droplet atomization mechanism [14] to circumvent the disadvantages of inkjet olfactory displays such as thermal injection, difficulty in downsizing the atomization mechanism, and complicated cleaning and maintenance [9].

Figure 1 illustrates the operation of the piezoelectric olfactory display [15]. This device uses a fan to blow a liquid fragrance that is atomized by a piezoelectric device built into a liquid fragrance tank to present the scent to the user. The piezoelectric device had a diameter of approximately 1 cm, and 100 micropores of 9 μm diameter were drilled in its center. Although the liquid fragrance in the liquid fragrance tank does not pass through the micropores owing to surface tension when no voltage is applied, it is atomized through the micropores by vibrations when a voltage is applied. The piezo element oscillated once every 10 μs, and approximately 167 pL of pure water atomization was observed with each oscillation.

A fan was employed to blow air over the atomized liquid fragrance, promote its volatilization of the liquid fragrance, and present the scent to the user.

A 3 mL capacity liquid fragrance tank was placed above the piezoelectric device and the fragrance in the tank was continuously ejected from the piezoelectric device. The tank, piezoelectric device, and the piezoelectric device holder at the bottom of the tank were removable to facilitate cleaning and maintenance. An experiment to measure the mass of purified water atomized 10 times for 10 s verified that the average injection mass was 0.17 g (standard deviation: 0.0077) and remained constant regardless of the number of atomization. Different types of fragrances have different viscosities,

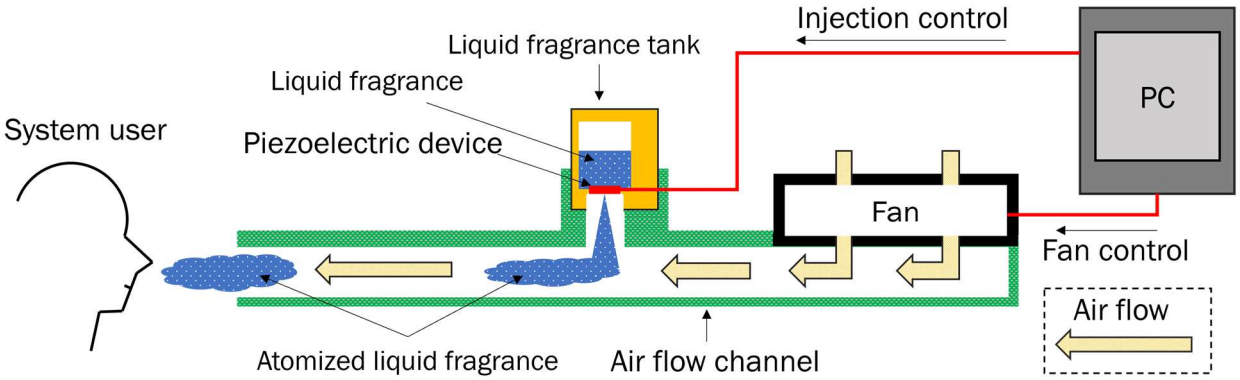

Figure 1: Cross-sectional image of piezoelectric olfactory display (side).

surface tensions, and other characteristics; therefore, fragrance solutions to be atomized in olfactory displays must be adjusted according to their composition.

2.2 Limitations of the Piezoelectric Device Olfactory Display

Our prototype's air flow channel has a cross section 20 mm high and 60 mm wide, which follows the structure of the inkjet olfactory display [9], [15]. To install the liquid fragrance tank, a 10 mm rise section was provided at the top of the air flow channel, and a cylindrical hole with a diameter and height of 15 mm and 15 mm, respectively, was created in the rise. The surface of the liquid fragrance tank was attached to the top of the raised section and atomization was directed vertically toward the bottom of the airflow channel. To prevent the piezoelectric device from being directly touched by hand, a 5 mm high dimple exists at the bottom of the liquid fragrance tank as a frame to protect the surface of the piezoelectric device, and a space for fixing the piezoelectric device exists above the frame. Therefore, the distance from the atomization position of the piezoelectric device to the bottom of the channel is 40 mm, which is equivalent to the atomized height of an inkjet olfactory display, and previous experiments with inkjet in olfactory displays, atomized substances are sufficiently vaporized in airflow channels [10]. Therefore, it was assumed that the atomized substance used in the piezoelectric olfactory display experiment vaporized immediately after ejection and did not remain as droplets on the wall surface.

However, the atomization mechanisms of inkjet and piezoelectric olfactory displays differ, including the composition of the liquid fragrance solution; hence, the vaporization of the atomized substance is also expected to differ.

We created an acrylic plate airflow channel with a height of 20 mm and a width of 60 mm to confirm the conditions in the airflow channel immediately after the atomization of droplets in the piezoelectric device olfactory display of our prototype [16]. We connected the liquid fragrance tank of our prototype method to the acrylic plate airflow channel and observed the inside of the airflow channel by capturing video images at the time of atomization. In the 0.3 s pulse injection experiment, purified water clearly left droplets over a wide area at the bottom of the channel, and it took approximately 10 s before the droplets were no longer visible. The droplets of the banana fragrance solution were not visible earlier than those of the purified water, with an average of 4.8 s. The time required for the droplets of the banana fragrance solution to disappear was approximately 10 s, whereas that of purified water was approximately 10 s. The results showed that the atomized substance adhered to the bottom surface of the conventional structure as droplets at the time of atomization of the banana liquid fragrance and purified water and evaporated later than after the system had finished atomizing them.

To accurately determine a person's scent detection threshold using a droplet-atomizing olfactory display, it is necessary to switch between odorless and attached states with a high degree of accuracy [9]. If the presentation state by the system is odorless but the subject is presented with a scent because of the above problem, the olfactory characteristics of the subject may not be measured correctly.

3 METHOD

To improve the volatilization of droplets observed in the piezoelectric olfactory display prototype, an experimental apparatus that allowed visual inspection of the inside of the display was constructed to confirm the conditions at the time of spraying. Based on the hypothesis that purified water is less likely to volatilize than fragrance solutions based on the residual time of droplets observed in the prototype described in Chapter 2, we created an experimental apparatus with a fixed channel width and changeable channel height in Experiment 1 to find a channel height at which droplet adhesion of purified water on the bottom surface is not observed. The channel height was determined to prevent droplets of purified water from adhering to the channel bottom. Because droplet adhesion was observed in the width direction in Experiment 1, Experiment 2 was conducted to determine a channel width that could be changed while keeping the channel height fixed at the height obtained in Experiment 1, so that no droplet adhesion could be observed on the sides. The presence or absence of droplets is determined by image processing, which highlights the droplets when visual observation is impossible. The effectiveness of the method was verified by spraying five fragrance solutions of different compositions on the final channel dimensions.

3.1 Experiment 1: Confirmation of the Required Air Flow Channel Bottom Distance During Purified Water Atomization

An experimental airflow channel was constructed using acrylic plates to determine the minimum distance at which a droplet was atomized by the piezoelectric device without contact with the bottom of the airflow channel. Figure 2 shows the configuration and dimensions of the experimental airflow channel.

In the experiment, the distance from the piezoelectric device to the bottom of the airflow channel was varied, and a video of the droplet atomization was recorded. Video images of the atomized droplets were captured and checked for the presence or absence of droplet adhesion at the bottom of the airflow channel. The threshold value of the bottom height for the presence or absence of deposits at the bottom of the airflow channel was defined as the minimum distance without contact with the bottom of the airflow channel when atomizing the droplets.

Previous studies have demonstrated that liquid fragrances containing ethanol or other solvents vaporize faster than purified water [16]. By determining the threshold of the bottom height relative to the purified water, liquid fragrances that could be used in the future can be considered. Therefore, only purified water was used in this experiment.

The experimental airflow channel employed a bottom surface whose height could be modified as desired; this is referred to as a movable floor in this study. The movable floor was an acrylic plate with the same dimensions as the bottom of the airflow channel, wrapped with vinyl tape at both ends and fixed in position by friction with the acrylic plate on the channel side. Therefore, the movable floor could be easily removed by changing the bottom height. To maintain constant conditions on the movable floor surface during continuous injection, each time the bottom height was changed, the surface was wiped with a paper rag moistened with purified water, and then dried again with a dry paper rag. While fixing the movable floor, the height of the installed surface was checked using a digital caliper, and a level was used to check the level at the part protruding from the channel prior to the experiment.

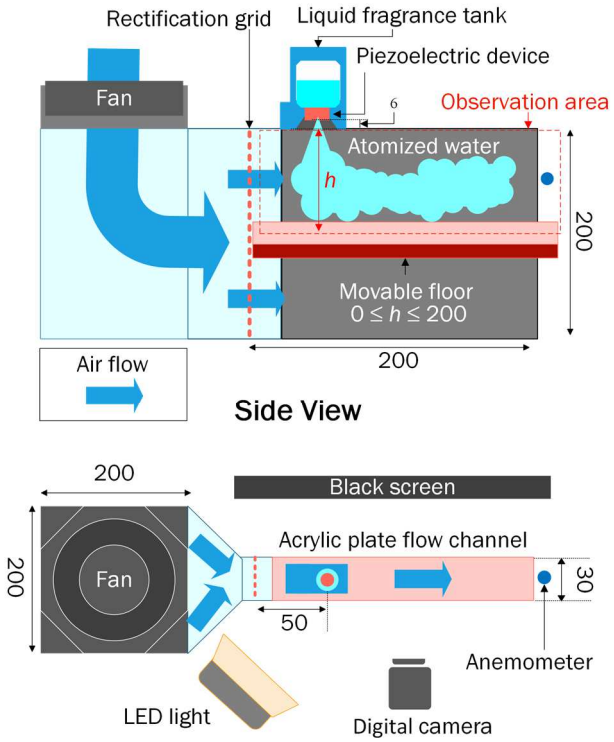

Figure 2: Structure of experimental channel for confirmation of the required airflow channel height (unit: mm).

The air velocity in the airflow channel during the droplet atomization experiment was 1.8 m/s, which was adopted in conventional experiments on inkjet olfactory displays [10].

A PWM-controllable PC fan was utilized to provide a constant airflow in the experimental airflow channel. The selection of the fan was based on the maximum airflow rate, and the fan was required to sufficiently satisfy the target air velocity over the entire experimental airflow channel cross section. Blowing air using rotating fans generated low velocity near the center of the air velocity distribution, asymmetrical bias, and turbulence. The airflow in the experimental airflow channel was stabilized to improve the reproducibility of the experimental results.

In this experimental airflow channel, a grid-like structure [17]-[18] used for rectification in the experimental wind tunnel was installed in the cross-section of the airflow channel, which flowed into the airflow channel from the fan mounting area. Previous experiments have demonstrated that the grid shape is effective in stabilizing the airflow in the airflow channels of piezoelectric olfactory displays when the pitch width, plate thickness, and open area ratio are 5 mm, 1 mm, and 60%, respectively [19]; in addition, the same parameters will be adopted in this study. The fan was mounted in the direction of the intake from the top of the experimental apparatus and perpendicular to the cross-section of the airflow channel to reduce the influence of the low-speed portion at the center of the fan. During the experiment, an anemometer was placed at the center of the cross-section, which was at the end of the experimental airflow channel, and the power of the fan was adjusted to achieve the target wind velocity while checking the wind velocity. The experiment was conducted only at wind speeds of 1.8 ± 0.03 m/s.

3.1.1 Experiment 1: Pre-Confirm of Wind Velocity Distribution in the Experimental Air Flow Channel

To verify the maximum air velocity and rectification effect in the experimental airflow channel, and to check whether the use of the movable floor significantly disturbed the air velocity distribution in the airflow channel cross-section, the air velocity distribution was measured at the vertical and horizontal centers of the cross-section at the airflow channel end when the experimental airflow channel height was h = 200 mm and h = 100 mm, with the movable floor at the output under the maximum airflow rate of the fan.

The experimental channel was created, and a 180 mm PC case fan "AP184i PRO" from Silver Stone was used for the fan, with PWM control using an Arduino uno 3. The experiment was conducted at a voltage of 12 V, which was

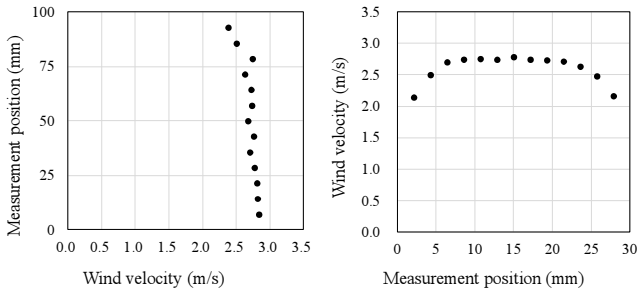

Figure 3: Wind speed distribution (h = 100 mm).

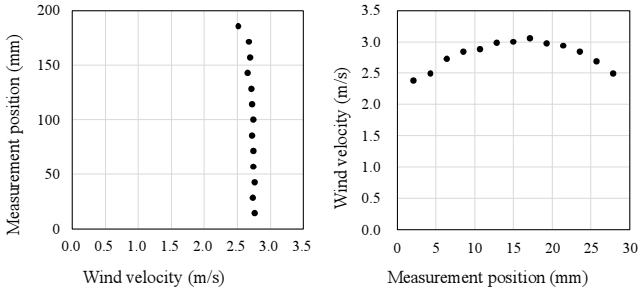

Figure 4: Wind speed distribution (h = 200 mm).

Table 1: Average wind velocity of channel cross-section

	Horizontal	Vertical	Horizontal	Vertical
h (mm)	100		200	
Mean (m/s)	2.61	2.7	2.8	2.7
SD (m/s)	0.21	0.12	0.21	0.06

the rated output of the fan, to determine the average wind speed at which a stable output was possible. The anemometer used was a KANOMAX Thermal Anemometer (Anemo Master Light Model 6006). The center of the anemometer element was captured for 10 s at each sampling point of the flow cross section, and the average

The value recorded per second was the measured value at each point. The anemometer element has a length of approximately 3 mm. During the measurement, the wind anemometer was oriented perpendicular to the direction in which the sampling point moved along the longitudinal axis such that the wind speed values were recorded as points.

In both cases, the vertical wind velocity distribution was almost flat, with an average of approximately 2.7 m/s, the horizontal wind velocity distribution was almost symmetrical, with the fastest near the center and gradually slowing as it approached the wall (Figs. 3-4). Table 1 presents the average wind velocity and standard deviation of the cross-section of the experimental airflow channel.

The obtained results indicate that the experimental airflow channel can be utilized for this experiment because the target air velocity of 1.8 m/s is sufficiently satisfied, and there is negligible turbulence in the air velocity distribution owing to the asymmetric flow caused by fan rotation and the influence of the movable floor.

3.2 Experiment 2: Confirmation of the Required Air Flow Channel Width During Purified Water Atomization

From the results of Experiment 1, no adhesion of purified water to the bottom of the channel was observed when the distance from the bottom of the channel to the piezoelectric element was at least 70 mm. In addition, droplet adhesion to the channel surface occurred regardless of the channel height when the width of the experimental channel was 30 mm. Therefore, to obtain a channel shape that does not allow droplet adhesion, this study describes a new experimental channel whose side width can be changed to obtain a channel width that does not allow droplet adhesion.

Based on the results of Experiment 1, the experimental channel shape was fixed at a channel height of 70 mm, and the total distance from the piezoelectric element to the bottom of the channel was 76 mm, including a 6 mm depression in the liquid fragrance tank. The channel width can be varied within the range 30-70 mm. Because the flow beyond a channel length of 200 mm could not be observed at the Experiment 1, a channel length of 300 mm was used in Experiment 2.

Using the PC fan connection module used in Experiment 1, we created a new acrylic plate flow channel and a rectifying flow structure. Two acrylic panels were placed parallel to each other in the channel and the distance between the panels was manually adjusted from the outside to change the channel width, which was used as a movable sidewall. When a prototype of the movable sidewall was fabricated using a 2-mm-thick acrylic plate, it was confirmed that the acrylic plate was warped, making it difficult to install it parallel to the wall. Because warpage was reduced using a 3-mm-thick acrylic plate, a 3-mm-thick acrylic plate was used for the movable sidewall in this method.

In a channel using only a rectifying grid with an aperture-to-area ratio of 60% and a grid spacing of 5 mm as the rectifying structure, the distribution was biased in the horizontal direction. This biased distribution can be attributed to the sudden change in the cross-sectional area of the flow path from the cross-section of a 200 mm high, 200 mm wide acrylic box connected to a fan to an experimental flow channel with a height of 70 mm and width of 80 mm. To weaken this effect, a bell-mouth shape was adopted, which enabled stable fluid intake by smoothly decreasing the cross-sectional area of the flow channel while connecting it from a wide space to a narrow duct. To prevent sudden contraction of the cross-sectional area of the experimental flow channel after it is narrowed by the movable sidewall at the connection between the bell mouth and the experimental flow channel, a hole is provided where the handle of the movable sidewall overlaps the cross-sectional area of the flow channel to allow air to pass through.

In this experimental channel, the wind velocity distributions at w = 70 mm and w = 35 mm were analyzed in the same way as described in Experiment 1 Both of mean wind speeds in horizontal directions were 2.51 m/s, the maximum wind speed differences at the horizontally symmetrical positions were 0.18 m/s and 0.14 m/s, and the standard deviations were 0.08 m/s and 0.17 m/s. The mean wind speeds in vertical

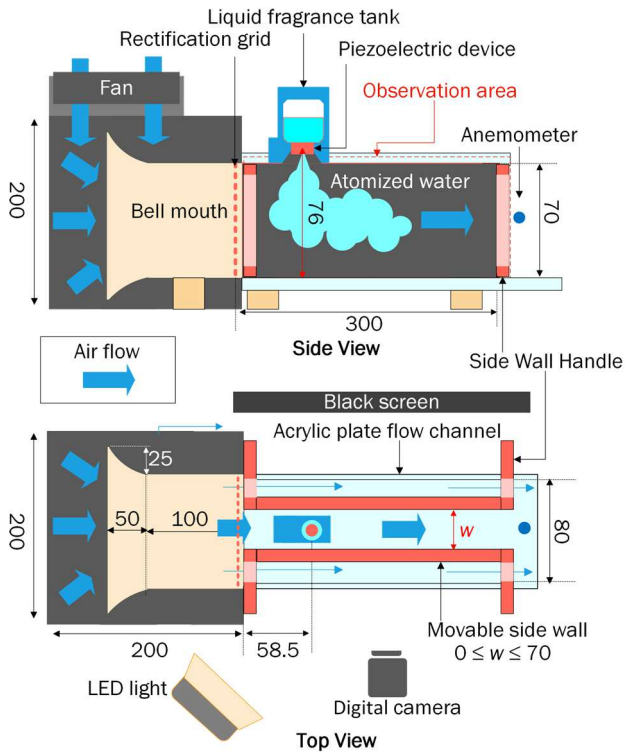

Figure 5: Structure of experimental channel for confirmation of the required air flow channel width (unit: mm).

directions were 2.57 m/s and 2.65 m/s, and the maximum wind speed difference at the vertical target position was 0.32 m/s and 0.30 m/s, with standard deviations of 0.08 m/s and 0.09 m/s. These wind velocity measurements did not reveal any extreme fluctuations in the wind velocity distribution due to changes in the channel width. The maximum wind velocity difference at the symmetrical horizontal position was 0.33 m/s at a channel width of 70 mm before the bell mouth was installed, whereas it was approximately half that after the bell mouth was installed. The wind velocity bias of each channel was considered acceptable and the experimental channels were used for the experiment.

Figure 5 shows an image of the experimental apparatus. Using this experimental channel, atomization experiments of pure water were conducted at 5 mm intervals at a channel width ranging from 30 mm to 70 mm. When the width of the flow channel was changed, the movable sidewalls were operated. Moreover, the width of the channel was measured with a digital caliper to confirm that the movable sidewalls were parallel to each other and that the experimental channel was horizontal using a leveler before conducting the experiment. In each channel-width experiment, the droplets were first atomized for more than 10 s and observed with the naked eye at a close distance of approximately 100 mm from the channel wall to check for abnormalities in the experimental equipment, droplet atomization, and droplet adhesion on the channel wall.

After confirmation, four sets of videos were captured from the side surface of the channel, with one set consisting of three consecutive droplet atomization for 1 s at 5 s intervals. An anemometer was used to check the wind speed at the center of the cross-section at the channel tip. Similar to the setup in Experiment 1, the camera was ready to start capturing the wind speed when it was 1.8 ± 0.03 m/s. Each set used different camera settings. In this experiment, full HD resolution (240 fps), 4 K resolution high dynamic range setting (30 fps), 4 K resolution normal capture (60 fps) brightness adjustment based on bright points, and 4 K resolution normal capture (60 fps) brightness adjustment based on dark points were used. After the experiment, the following were confirmed based on the results for each channel width: No obvious droplet adhesion was observed by naked-eye inspection. In each of the 12 videos of droplet atomization, the target frame was captured 0.17 s after the end of atomization when an object moving at 1.8 m/s had traveled the full distance of 300 mm from the end of ejection.

When a channel width that simultaneously satisfied these criteria was obtained in the atomization experiment with purified water, the atomization experiments of solutions with five different water-soluble fragrances (banana, lemon, rose, vanilla, and blueberry) were conducted at the minimum channel width in the same manner as the method used for purified water.

The atomizing solution for these experiments was prepared using commercially available water-soluble flavoring agents for food additives from Marugo Corporation, as described in our prototype. For the fragrance solution, dilute the water-soluble fragrance of each flavor with purified water, obtain a fragrance component to be 5% by mass. The substances and amounts of the flavor components of each flavor used in the experiment are not disclosed. Therefore, based on the mass of the indicated organic solvent, the difference between the overall mass and the mass of the organic solvent was assumed to be the mass of the flavor components, and the ratio of the fragrance solutions mixed with purified water for each flavor was determined. Table 2 lists the ratios of the solutions used in the experiments. Of the five fragrance solutions selected for the experiment, two (banana and lemon) have been used in a previous study. Among the newly prepared fragrance solutions, we selected three (rose, vanilla, and blueberry) that differed significantly from those used in the previous study in terms of the physical properties (surface tension and viscosity) and composition of the fragrance solutions. If this experiment shows similar to those obtained for purified water, the experimental channel width and channel height can be considered appropriate shape parameters for the design of a rectangular channel to be used in novel piezoelectric olfactory displays with a central air velocity of 1.8 m/s at the tip channel cross-section.

Table 2: Component ratios of atomization solutions (%).

	Vanilla	Rose	Banana	Blueberry	Lemon
Fragrance Components	5.00	5.00	5.00	5.00	5.00
Ethanol	2.24	4.00	5.11	5.00	7.92
Glycerol	0.22	1.00	1.14	-	0.97
Propylene Glycol	-	-	0.11	2.50	-
Water	92.54	90.00	88.64	87.50	86.11

3.3 Image Processing for Improved Visibility of Droplets

To confirm the presence or absence of droplet adhesion on the atomized target and channel wall, a background subtraction method was used to visualize the atomized target, using the frame before the start of droplet atomization as a background image. The contrast-enhanced image was then observed using histogram flattening to confirm the absence of droplet atomization-caused droplet adhesion to the channel. For image processing, Python3 and Open CV 4.6.0 library were used.

The "cvtColor method" with the COLOR_BGR2GRAY parameter was used to convert the target frame and background images to grayscale and the RGB values of the pixels to luminance values. The difference between the luminance values of the gray scaled target frame and the background image is obtained using the "absdiff method." This method only visualizes areas in which the luminance values change between the target and background images.

Histogram averaging was performed on the images obtained using the background subtraction method to enhance the contrast and improve the visibility of the observed object. The method uses the "clahe method" to perform adaptive histogram averaging on an image obtained by subtracting the background image from the target frame.

4 RESULTS

4.1 Experiment 1: Confirmation of the Required Air Flow Channel Bottom Distance During Purified Water Atomization

An experimental airflow channel was fabricated using a 3D printer and an acrylic sheet.

Figure 6 shows the atomization at h = 34 mm. A digital camera was positioned at the center of the screen at an angle that captured the entire movable floor surface, and any droplet adhesion on the bottom of the channel during purified water spraying was illuminated by white LED light adopted as illumination and visualized in white.

Figures 7-9 show present the experimental results for h = 34, 63, and 64 mm, respectively, during 1 s of purified water

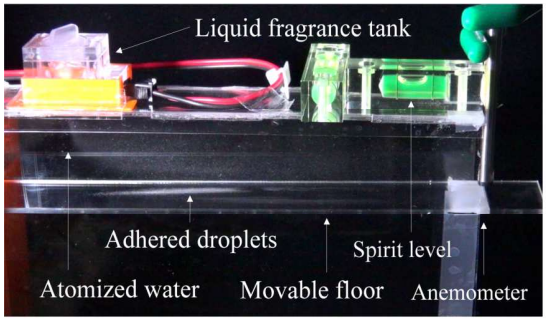

Figure 6: Illustration of experimental results (h = 34 mm).

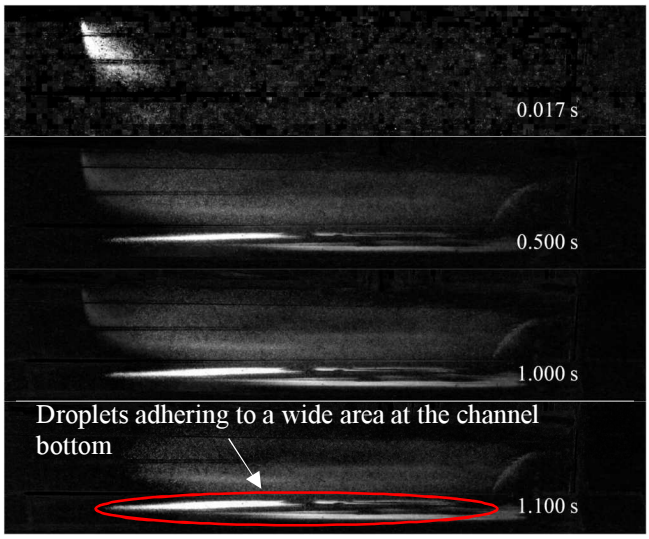

Figure 7: Experimental results (h = 34 mm, Color difference from 0 s and after contrast adjustment, Clipping only in air flow channel).

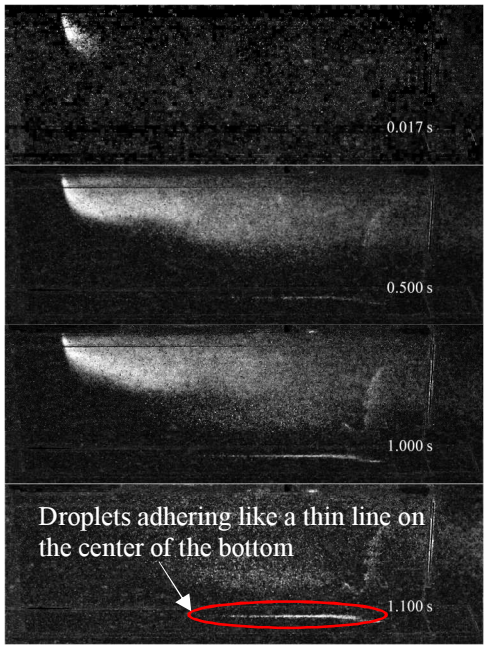

Figure 8: Experimental results (h = 63 mm, Color difference from 0 s and after contrast adjustment, Clipping only in air flow channel).

atomization, where; the time series changed when the atomization start frame was set to 0 s.

These images were clipped only inside the airflow channel, and the difference in color values between the atomizing start frame and each frame was determined using the method of section 3.3. The color values were output only for the areas that changed from the initial frame; and the areas that did not change were output in black. At h = 34 mm (in Fig. 7), droplet adhesion was clearly observed over a wide area of the movable floor surface. The droplets remained at the bottom of the air flow channel for 1.1 s after atomization was completed, and the atomized substance flowed out of the airflow channel. As shown in Fig. 8, at h = 63 mm, linear droplet adhesion was observed at the center of the movable

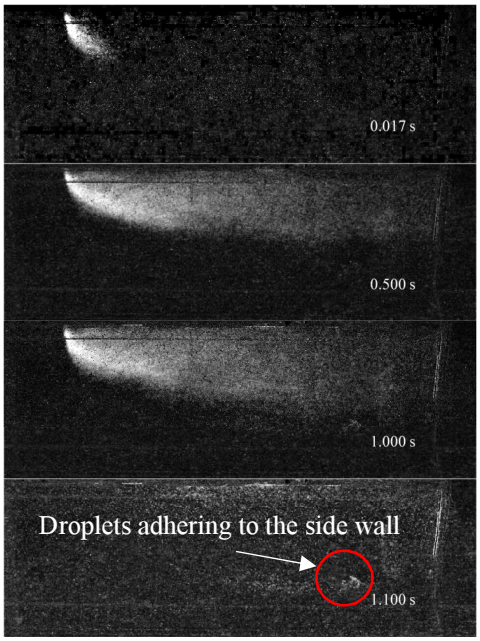

Figure 9: Experimental results (h = 64 mm, Color difference from 0 s and after contrast adjustment, Clipping only in air flow channel).

floor in front of the airflow channel in the form of a thin line. In Fig. 9, h = 64 mm, the atomized substance flowing in the channel was confirmed; however, no bottom adhesion was observed, and the same result was obtained in six subsequent trials conducted for confirmation.

In all cases, however, droplet adhesion was observed on a surface on the channel side 1.1 s after the end of injection, when the 1.8 m/s wind velocity should have sufficiently ejected substances out of the channel.

This means that the 30 mm channel width of the experimental channel was insufficient to prevent droplet adhesion to the channel sides.

4.2 Experiment 2: Confirmation of the Required Air Flow Channel Width During Purified Water Atomization

An experimental channel with a variable width was created, and purified water atomization experiments were conducted. Similar to the setup of Experiment 1, a shape model of the experimental channel was created using Autodesk's "Fusion360" software. A bell mouth was made from the shape model using a 3D printer ("Raise 3D E2") with a PLA filament as the material. The experimental flow channel, rectifying grating, and movable sidewalls were fabricated by cutting acrylic sheets using a laser cutting machine based on the shape data. The parts were fixed with an acrylic adhesive and sealed with vinyl tape to prevent air leakage from the joints.

In previous experiments, droplet atomization in liquid fragrance tanks was found to fluctuate owing to the deterioration of the piezoelectric element, the presence of dirt, and poor contact between the connection terminals. The droplet-atomizing performances of the four liquid fragrance tanks were compared. The liquid fragrance tank with the highest average atomizing mass and the lowest coefficient of variation was selected for use in the experiment. The average atomizing mass of purified water droplets in the liquid

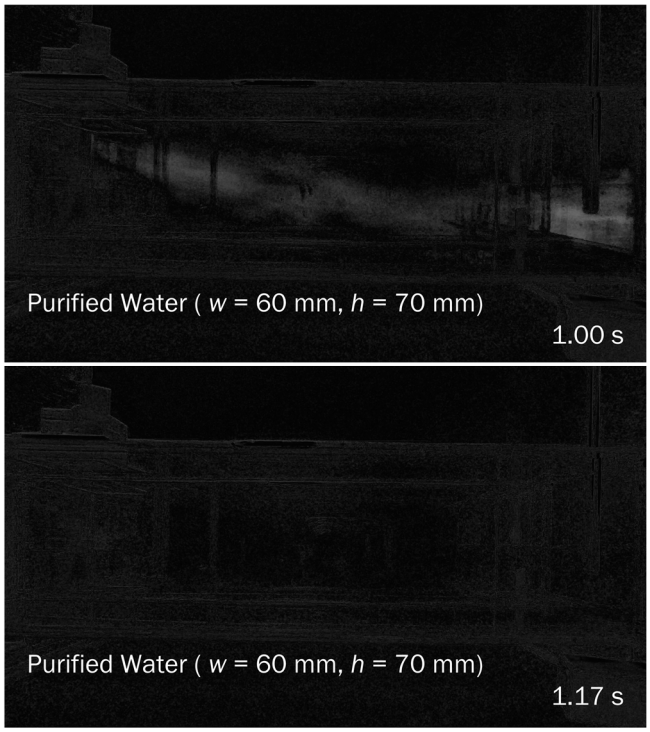

Figure 10: Side view of experimental results of purified water atomization (images obtained by Contrast Limited Adaptive Histogram Equalization for background subtraction before and after atomization).

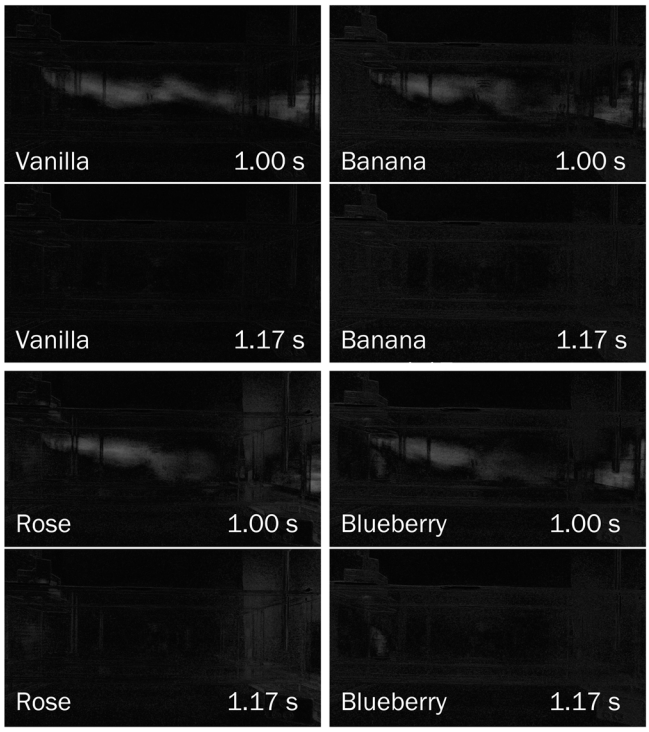

Figure 11: Side view of experimental results of four fragrance solution atomization (w = 60 mm, h = 70 mm).

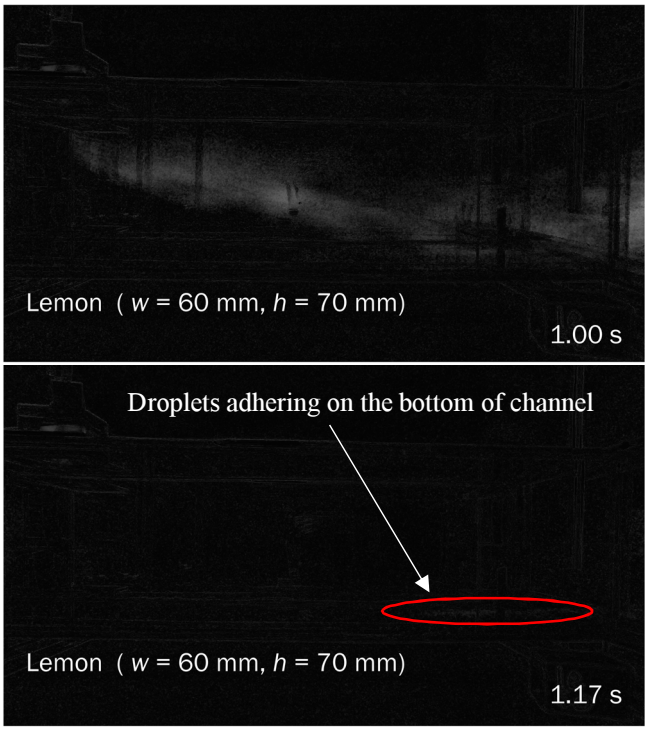

Figure 12: Side view of experimental results of the lemon fragrance solution atomization.

fragrance tank used in the experiment was 2.08 mg/s, with a standard deviation of 0.08 mg/s and a coefficient of variation of 3.60%. The following results were obtained using one of the liquid fragrance tanks. A piezoelectric element and a liquid fragrance tank containing purified water were placed in the experimental channel such that the piezoelectric element surface was horizontal and fixed with vinyl tape to prevent displacement during the experiment.

During the filming, the lights were turned off, the area around the experimental apparatus was covered with a blackout curtain to prevent the influence of flickering natural or fluorescent light, and a small LED light source was used for video recording. Purified water atomization experiments were conducted using the experimental setup described above. A DJI "OSMO ACTION" camera was used to capture images of the experimental flow channel while switching the camera settings for each experiment. The temperature and humidity at the start of the experiment were 21.6°C and 20.7%, respectively.

The results of the purified water atomization experiments are presented below. Naked-eye inspection of the channel wall during 10 s of purified water atomization revealed numerous small droplets on the channel wall and top surface at the center of the channel at w = 30-35 mm. The small droplets that adhered to the wall volatilized immediately after contact. At w = 40-55 mm, droplet adhesion to the top surface of the channel was no longer observed. Small droplets were observed to contact the channel-side surface in the range of 100-150 mm from just below the liquid fragrance tank toward the channel tip and volatilized immediately after contact. The frequency of the droplet contacts with the channel-side surface decreased as the channel width increased. At w = 60-70 mm, almost no droplet contact was observed by naked-eye inspection. The target frame was captured 0.17 s after droplet atomization by applying image processing to a video captured at w = 60 mm. Figure 10 shows the results after image processing just before the end of 1 s of purified water atomization and 0.17 s after the atomization.

Next, experiments were conducted at w = 60 mm by atomizing the solutions of five water-soluble fragrances (banana, lemon, rose, vanilla, and blueberry).

No droplet adhesion to the channel sidewall was observed for any of the liquid fragrance solutions, either with the naked eye or in the target frames of the video after image processing. However, droplet adhesion to the bottom of the channel was observed in the 11 atomization of the lemon fragrance solution. White streaky adherent droplets were observed in the center of the bottom of the channel from 150 mm to 200 mm from the atomizing start position to the end of the channel after ≥ 0.17 s. Figures 11-12 show the results after image processing just before the end of 1.00 s of liquid fragrance solutions atomization and 0.17 s after the atomization.

5 ANALYSIS

5.1 Experiment 1: Confirmation of the Required Air Flow Channel Height at the Time of Purified Water Atomization

The airflow channel height of the conventional piezoelectric olfactory display (h = 34 mm) was insufficient because of the large number of droplets adhering to the bottom surface. Bottom adhesions were observed at $h \leq 63$ mm; however, no bottom adhesions were observed at $h > 64$ mm even after repeated atomization. The required air flow channel bottom distance at the time of purified water atomization at a flow velocity of 1.8 m/s, when vibrating at 100 kHz using a piezoelectric device with 100 micro-holes of 9 μm, was verified to be 70 mm, including the dimple in the liquid fragrance tank.

In all cases, contact was observed on the sides during atomization at an 30 mm airflow channel width.

5.2 Experiment 2: Confirmation of the Required Air Flow Channel Width at the Time of Purified Water Atomization

Experiments using purified water and four kinds of except lemon fragrance solution showed that no droplet residue was observed on the wall surface when droplets were atomized by using a channel with geometry parameters of $w \geq 60$ mm and $h \geq 70$ mm. This confirms that for water-soluble liquid flavorings other than lemon flavorings used in the experiment, there are no visible droplets in the channel at 0.17 s after the end of spraying, due to the obtained channel shape parameters, rather than the conventional parameters of w = 60 mm and h = 34 mm. Compared to the 4.8 s required for the volatilization of banana flavor droplets observed in the prototype, the residual time of the droplets in the channel was reduced to approximately 3.5%. The ambient fragrance during all the atomization experiments using water-soluble liquid fragrances qualitatively indicated that each fragrance could be represented by the piezoelectric olfactory display.

However, the lemon fragrance solution used in this experiment in a channel with a flow channel more than 200 mm from the atomizing point may cause adhesion problems at the bottom of the channel.

In this experiment, we considered why bottom adhesion occurred only with the lemon fragrance solution. Considering the volatility of the liquid from the boiling points under standard atmospheric pressure of the components of the lemon fragrance solution, glycerin (boiling point 290°C), which has the highest boiling point among the known components, was present at approximately 1%. However, under the same conditions, no adhesion to the bottom surface was observed for rose and banana fragrance solutions containing similar amounts of glycerin. The lemon fragrance solution contained the highest amount of ethanol (boiling point 78.37°C) and the lowest amount of water (boiling point 100°C) among the tested solutions. The unique flavor components of the lemons used in this study are not disclosed. Therefore, it is difficult to explain the reason for droplet adhesion to the bottom surface because of the volatility of the ingredients. In the future, it will be necessary to conduct experiments using lemon fragrance solutions with known ingredients and to measure the actual volatilization time of the fragrance solutions.

The effect of specific gravity of the fragrance solution was also considered. The different specific gravities of the droplets may cause differences in the diffusion range owing to the effect of gravity. All video frames for a certain period of time during atomization were superimposed and added together to visualize the diffusion range of the atomized droplets. This may explain the difference in the diffusion range of each fragrance solution, and the relationship between the specific gravity of the fragrance solution and the diffusion range of the droplet, which may explain the lower adhesion of the lemon fragrance.

In the movie taken from the experiment using purified water with a channel width of w = 30-55 mm, where naked-eye inspection confirmed droplet adhesion, droplet adhesion was not as clearly identified as in Experiment 1. First, there was a difference in the attachment method of the liquid fragrance tank between Experiment 2 and Experiment 1. In Experiment 2, the liquid fragrance tank was fixed to the experimental channel using vinyl tape to maintain the direction of atomization of the liquid fragrance tank perpendicular to the bottom of the channel. Therefore, in the results of Experiment 1, where droplet adhesion was observed on the side surface of the flow channel, it is possible that a tilt existed in the atomizing direction of the liquid fragrance tank, and droplets were sprayed on one side of the channel. Second, the effect of illumination on the visualization of droplets may differ from that of the experimental channel used in Experiment 1 because one more acrylic plate passes between the channel wall with attached droplets and the video equipment owing to the movable sidewalls. It indicates the need for improved lighting and experimental filming conditions.

6 CONCLUSION

To improve the performance of the prototype piezoelectric olfactory display, experiments were conducted to determine the channel height and width at which sprayed droplets were no longer visible in the channel. To correct the bias in the wind velocity distribution identified during the process of developing the experimental channel, data from wind tunnel production were used to obtain a stable wind velocity distribution with reduced bias using a rectifying grid and upon shrinkage of the channel cross-section. Using an experimental flow whose height could be changed, we conducted a purified water atomization experiment at a central wind velocity of 1.8 m/s at the channel tip, similar to the conditions of the conventional method. The results of the naked-eye inspection and experimental filming indicated no droplet adhesion to the channel bottom when the channel height was 64 mm or when the distance from the channel bottom to the piezoelectric element was 70 mm. An experimental channel with a variable width was used to conduct the purified water atomization experiment.

No droplet adhesion was observed on the channel-side surface when the channel width was 60 mm through video and visual observations. In the experimental channel with geometric parameters of w = 60 mm and h = 70 mm, where no droplet adhesion was observed in purified water, solutions of five liquid fragrances (banana, lemon, rose, vanilla, and blueberry) were atomized, and no droplet adhesion was observed on the channel sidewall, similar to the results for purified water.

However, in the lemon-flavored solution used in this study, droplet adhesion to the bottom of the channel was observed in all results. This indicates that in an experiment to determine the appropriate channel height for an olfactory display, only atomizing purified water and checking for droplet adhesion to the bottom are not sufficient to draw a conclusion. In the future, it will be effective to use this experimental flow channel to set the fragrances to be used in advance, determine the appropriate shape sufficient to use them, and check the effects of changing the mixture components of the fragrance solution to adapt to the set channel shape.

In addition, the piezoelectric olfactory display qualitatively presented the liquid fragrances used in the experiment. These experimental results indicate that for applications involving the liquid fragrance used in the experiment, other than the lemon solution, the residual droplets on the channel wall can be reduced using a channel width of $\geq$ 60 mm and channel height of $\geq$ 70 mm when designing a new appropriate channel structure. Future experiments using new fragrances will confirm whether the shape parameters obtained in this study are applicable to a wide variety of liquid fragrances. Based on the shape parameters determined in this study, we will create a prototype of a new piezoelectric olfactory display and compare with an inkjet olfactory display using a test subject.

REFERENCES

[1] M. L. Heilig, Sensorama Simulator, U.S.Patent 3050870 (1962).

[2] T. Narumi, T. Kajinami, S. Nishizaka, T. Tanikawa, and M. Hirose, “Pseudo-gustatory display system based on cross-modal integration of vision, olfaction and gustation”, 2011 IEEE Virtual Reality Conference, pp.127-130 (2011).

[3] Y. Yanagida, "Projection based olfactory display with nose tracking", VR '04: Proceedings of the IEEE Virtual Reality 2004, pp.43-50 (2004).
[4] T. Yamada, S. Yokoyama, T. Tanikawa, K. Hirota, and M. Hirose, "Wearable Olfactory Display: Using Odor in Outdoor Environment", IEEE Virtual Reality Conference (VR 2006), pp.199-206 (2006).
[5] C. J. 4dplex, 4DX SIGNATURE EFFECTS, https://www.cj4dx.com/aboutus/aboutus.php (Accessed: 20-Apr-2023).
[6] A. Mochizuki, T. Amada, S. Sawa, T. Takeda, S. Motoyashiki, K. Kohyama, M. Imura, and K. Chihara, "Fragra: a visual-olfactory VR game", ACM SIGGRAPH 2004 Sketches, p.123 (2004).
[7] Y. Yanagida, "A survey of olfactory displays: Making and delivering scents", SENSORS, 2012 IEEE, pp.1-4 (2012).
[8] Y. Bannai, "Olfactory display using piezoelectric element", in Odor sensing, analysis and its visualization and quantification, Technical Information Institute, pp.518-529 (2020). (in Japanese)
[9] S. Sugimoto, D. Noguchi, Y. Bannnai, and K. Okada, "Ink Jet Olfactory Display Enabling Instantaneous Switches of Scents", Proceedings of the 18th ACM International Conference on Multimedia, pp.301-310 (2010).
[10] A. Kadowaki, J. Sato, Y. Bannai, and K. Okada, "Measurement and Modeling of Olfactory Responses to Pulse Ejection of Odors", Journal of Japan Association on Odor Environment, Vol.39, No.1, pp.36-43 (2008).
[11] A. Kadowaki, J. Sato, Y. Bannai, and K. Okada, "Presentation Technique of Scent to Avoid Olfactory Adaptation", 17th International Conference on Artificial Reality and Telexistence (ICAT 2007), pp.97-104 (2007).
[12] D. Noguchi, S. Sugimoto, Y. Bannai, and K. Okada, "Time Characteristics of Olfaction in a Single Breath", Proceedings of the SIGCHI Conference on Human Factors in Computing Systems, pp.83-92 (2011).
[13] A. Aruga, Y. Bannai, and T. Seno, "Investigation of the Influence of Scent on Self-Motion Feeling by Vection", International Journal of Informatics Society, Vol.11, No.2, pp.65-73 (2019).
[14] Q. Yan, J. You, W. Sun, Y. Wang, H. Wang, and L. Zhang, "Advances in Piezoelectric Jet and Atomization Devices", Applied Sciences, Vol.11, No.11, p.5093 (2021).
[15] S. Nakamura, Y. Bannai, "Development of An Olfactory Display Using a Piezoelectric Element and Measurement of Olfactory Detection Threshold", VRSJ Research Report, Vol.25, No.SBR-1, pp.1-6 (2020). (in Japanese)
[16] Y. Seta, M. Makino, Y. Bannai, and M. Hattori, "Proposal of Air-Flow Channel Structures of The Olfactory Display Using the Piezoelectric Element Considering Fluid Behavior", VRSJ Research Report, Vol.27, No.SBR-1, pp.9-14 (2022). (in Japanese)
[17] M. Tachibana, and K. Yoshida, "Energy Loss due to Honeycomb in a Pipe Flow", Memoirs of the Faculty of Engineering, Fukui University, Vol.43, No.1, pp.103-108 (1995). (in Japanese)
[18] Y. Kohama, "Optimum Screens for Turbulence Reduction in Wind Tunnels", Journal of Japan Society of Fluid Mechanics Nagare, Vol.9, No.1, pp.19-33 (1990). (in Japanese)
[19] Y. Seta, N. Mori, M. Makino, Y. Bannai, and M. Hattori, "Comparison of Rectification Effects of Grid Shapes in an Air-Flow Channel for Droplet Spray Olfactory Displays", Proceedings of the 84th National Convention of IPSJ, p.2F-05 (2022). (in Japanese)

(Received: February 1, 2023)
(Accepted: July 5, 2023)

Yohei Seta He is a Doctor Course Student of Graduate School of Science and Engineering at Chuo University. He received a Bachelor of Media Science and a Master of Media Science from Tokyo University of Technology. in 2009 and 2011, respectively. His research interests include real-time computer graphics, virtual reality, computational fluid dynamics.

Mitsunori Makino received his B.E, M.E and Dr. Eng in Electronic Communication Engineering from Waseda University in 1987,1989 and 1992, respectively. He was a research assistant at Waseda University from 1991 to 1992. He joined Chuo University in 1992, and has been a full professor of the Faculty of Science and Engineering, Chuo University since 2004. His research interests are mainly in technologies and their applications in CG, XR and visualization. His activities also include engineering education. He is currently the director and the committee chairperson of the Criteria in Japan Accreditation Board of Engineering Education.

Yuichi Bannai He is a professor of Department of Information Media at Kanagawa Institute of Technology, Japan. He received a BE and a ME from Waseda Univ. in 1978 and 1980, respectively, and joined Canon Inc. in 1980. He also received MS from Michigan State University in 1988, and Ph D from Keio University in 2007. His research interests include human five senses interaction, artificial intelligence, and virtual/augmented reality. He is a member of ACM, IEEE CS, IPSJ, Japanese Society for AI, and Virtual Reality Society of Japan (VRSJ).

Motofumi Hattori He is a professor of Department of Information Media at Kanagawa Institute of Technology, Japan. He received a Master of Science from Kobe University in 1991. He received a Master of Engineering from Kobe University in 1993. He received a Doctor of Engineering from Kobe University in 2000. His research interests include Game Amusement, Virtual Reality, Computational Fluid Dynamics, and Statistical Physics. He is a member of Game Amusement Society of Japan, Virtual Reality Society of Japan, IPSJ, The Japan Society for Computational Engineering and Science, and The Japan Society of Fluid Mechanics.